



OPEN

Roles for *Tbx3* in regulation of two-cell state and telomere elongation in mouse ES cellsSUBJECT AREAS:
EXTRACELLULAR
SIGNALLING MOLECULES
EMBRYONIC STEM CELLSJiameng Dan¹, Minshu Li¹, Jiao Yang¹, Jiaojiao Li¹, Maja Okuka², Xiaoying Ye¹ & Lin Liu¹Received
10 October 2013Accepted
26 November 2013Published
13 December 2013Correspondence and
requests for materials
should be addressed to
L.L. (liulin@nankai.edu.
cn)¹State Key Laboratory of Medicinal Chemical Biology; Department of Cell Biology and Genetics, College of Life Sciences, Nankai University, Tianjin 300071, China, ²Department of Obstetrics and Gynecology, University of South Florida College of Medicine, Tampa, FL 33612, USA.

Mouse embryonic stem (ES) cell cultures exhibit heterogeneity and recently are discovered to sporadically enter the 2-cell (2C)-embryo state, critical for ES potency. *Zscan4* could mark the sporadic 2C-state of ES cells. However, factors that regulate the *Zscan4*⁺/2C state remain to be elucidated. We show that *Tbx3* plays a novel role in regulation of *Zscan4*⁺/2C state. *Tbx3* activates 2-cell genes including *Zscan4* and *Tcstv1/3*, but not vice versa. Ectopic expression of *Tbx3* results in telomere elongation, consistent with a role for *Zscan4* in telomere lengthening. Mechanistically, *Tbx3* decreases Dnmt3b and increases Tet2 protein levels, and reduces binding of Dnmt3b to subtelomeres, resulting in reduced DNA methylation and derepression of genes at subtelomeres, e.g. *Zscan4*. These data suggest that *Tbx3* can activate *Zscan4*⁺/2C state by negative regulation of DNA methylation at repeated sequences, linking to telomere maintenance and self-renewal of ES cells.

Mouse ES cells are derived from the inner cell mass (ICM) of blastocysts and thought to be functionally equivalent to inner cell mass (ICM), harboring similar gene expression patterns compared to ICM cells¹. Mouse ES cells are featured with pluripotency and self-renewal^{2,3}. Another unique hallmark of mouse ES cells is their ability to defy cellular senescence and maintain exceptional genomic stability undergoing many cell divisions compared to other cell types⁴. It is also to note that ES cell cultures are a heterogeneous mixture of metastable cells with fluctuating expression of genes such as *Zscan4*, *Zfp42/Rex1*, *Rest*, *Nanog*, *Stella* (also known as *Dppa3*) and *Esrrb*^{1,5,6}. Furthermore, mouse ES cells fluctuate with activation of 2-cell embryo specific genes (2C-genes) and endogenous transposable element (TE) activities⁷, suggesting that ES cells in the 2C-state might resemble the totipotent zygotes/2C-stage embryos. In this regard, the 2C-state was postulated as a “super” state of ES cells⁸. Interestingly, a large number of the genomic locations encoding the 2C-genes are enriched for TE-derived sequences. In addition, the 2C-genes are co-regulated with TEs⁷.

Zscan4, expressed specifically in 2-cell embryos and transiently in sporadic ES cells (1–5%) at any given time, marks a transient 2C-state of mouse ES cells⁴ and is required for preimplantation embryonic development and lengthening telomeres promptly by recombination-based mechanisms and maintaining genomic stability^{4,9,10}. *Zscan4*⁺ and *Zscan4*⁻ ES cells can interconvert to each other and nearly all ES cells activate *Zscan4* at least once during nine passages⁴. Interestingly, *Zscan4* can activate early embryonic genes, including 2C-genes, and maintain genomic stability during generation of induced pluripotent stem (iPS) cells^{11,12}. Moreover, *Zscan4* levels affect pluripotency of ES cells¹³. Without intermittent activation of *Zscan4*, embryos delay preimplantation development and ES cells lose their ability to proliferate indefinitely⁹, suggesting that the equilibrium between the 2C-state and canonical ES state is essential for proper embryonic development. However, how *Zscan4*/2-cell state is regulated in ES cell cultures remains elusive, and presumably multiple regulators may be involved in the regulation of 2-cell state. Here, we have identified *Tbx3* as an epigenetic regulator of *Zscan4*⁺/2C state in ES cell cultures.

Results

***Tbx3* is upregulated in 2C-state of mouse ES cell cultures.** We hypothesized that the 2C-state regulators may exist within *Zscan4*⁺ cells/2-cell state, and that *Zscan4*⁺ cells contain factors regulating *Zscan4*⁺ cell status. To search for factors that potentially regulate 2C-state, we thought to select genes prominently up-regulated in 2-cell embryos and 2C::tomato⁺ mouse ES cells compared to oocytes and 2C::tomato⁻ mouse ES cells, respectively⁷. *Zscan4*, previously identified as a specific marker for two-cell embryo and mouse ES cells, highly expressed in 2C::tomato⁺ mouse ES



cells while absent in *2C::tomato*⁻ mouse ES cells, can faithfully represent the 2C-state of mouse ES cells^{4,7,9}. We also generated a *Zscan4* promoter-driven EGFP (*Zscan4*-EGFP) ES cell line shown to closely recapitulate the endogenous *Zscan4* expression⁴. *Zscan4* was only expressed in a small subset of ES cells (Fig. 1a). ES cells were then sorted into *Zscan4*⁺ and *Zscan4*⁻ populations by flow cytometry, the

Zscan4-EGFP⁺ 2C-cell pool was limited to 1–5% (Fig. 1b), consistent with the recent report⁴. The selected genes including *Tcstv1*, *Tcstv3*, *Dub1*, *Dazl*, *Ott* and *Tbx3* expressed at much higher levels in sorted *Zscan4*⁺ than in *Zscan4*⁻ ES cells (Fig. 1c). These genes might be the potential regulators of *Zscan4*⁺/2C-state or downstream targets of *Zscan4*⁺/2C-state.

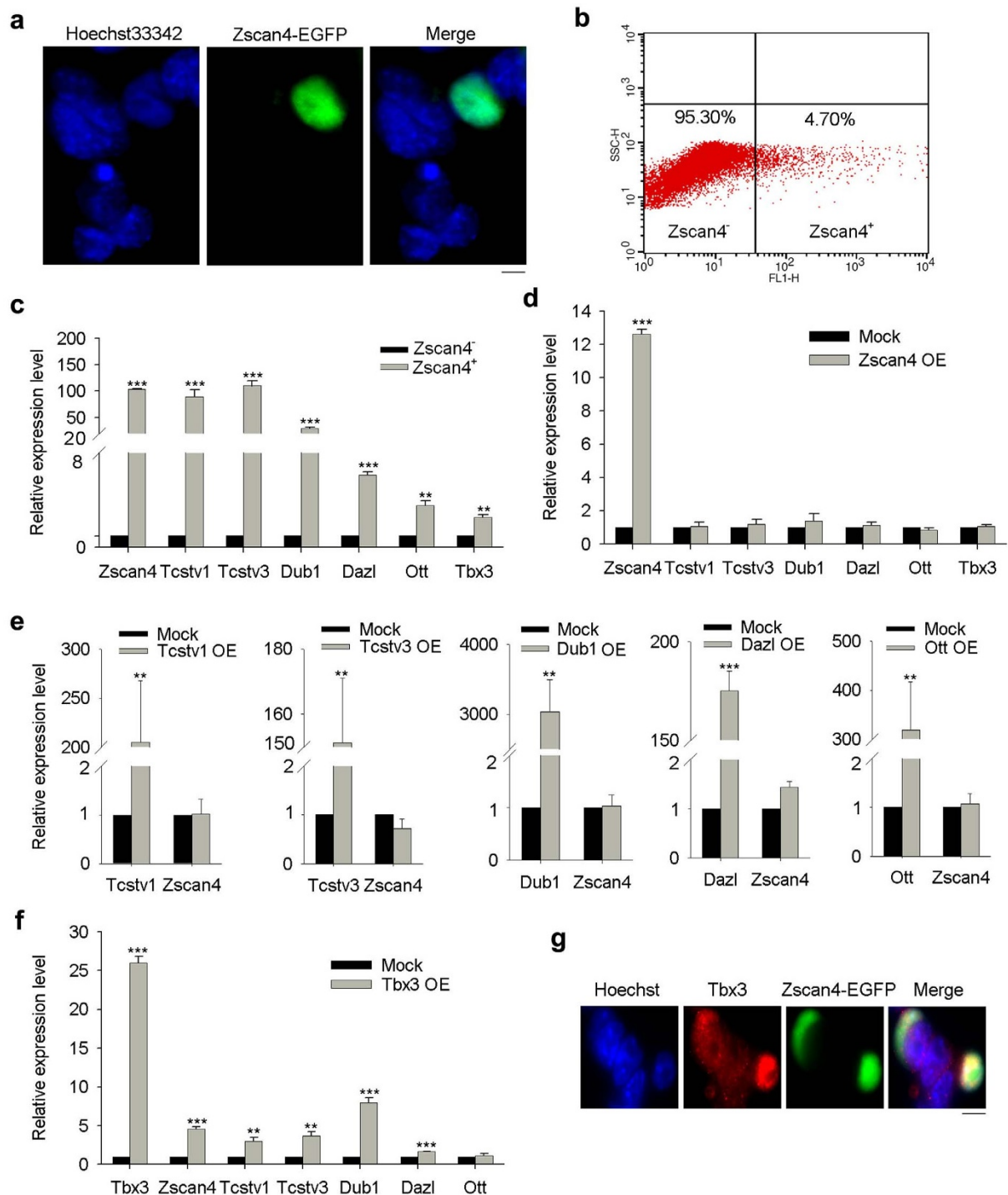


Figure 1 | *Tbx3* regulates *Zscan4*/2C genes. (a) *Zscan4*-promoter-driven EGFP reporter in J1 ES cells shows that only a subpopulation of ES cells express *Zscan4* at a given time. Nuclei stained by Hoechst 33342. Scale Bar = 5 μm. (b) *Zscan4*⁺ and *Zscan4*⁻ ES cells were sorted by FACS. (c) *Zscan4*, *Tcstv1*, *Tcstv3*, *Dub1*, *Dazl*, *Ott* and *Tbx3* up-regulated in *Zscan4*⁺ ES cells compared to *Zscan4*⁻ ES cells. (d) Over-expression of *Zscan4* in ES cells did not alter expression of above six genes. (e) Over-expression of *Tcstv1*, *Tcstv3*, *Dub1*, *Dazl* and *Ott* in ES cells did not change *Zscan4* expression. (f) *Tbx3* over-expression in ES cells up-regulated expression of *Zscan4*, *Tcstv1*, *Tcstv3* and *Dazl*. (g) Immunostaining of *Tbx3* (red) in *Zscan4*-EGFP ES cells. Nuclei stained by Hoechst 33342. *Zscan4* positive (2C-state) ES cells showed higher expression of *Tbx3*. Scale Bar = 10 μm. Error bars indicate mean ± SEM (n = 3). **, p < 0.01; ***, p < 0.001, compared to controls.



To determine whether the six genes are downstream targets of *Zscan4*⁺/2C-state, we over-expressed *Zscan4* in ES cells for 48 h and found that expression of genes *Tcstv1*, *Tcstv3*, *Dub1*, *Dazl*, *Ott* and *Tbx3* did not differ between *Zscan4* over-expressed ES cells and the mock ES cells (Fig. 1d), suggesting that *Zscan4* itself does not activate *Tcstv1*, *Tcstv3*, *Dub1*, *Dazl*, *Ott* and *Tbx3*. To examine whether these six genes positively regulate *Zscan4*/2C-state in mouse ES cells, we transiently over-expressed each of the six genes alone in mouse ES cells, and looked at expression levels of *Zscan4*. Overexpression of *Tcstv1*, *Tcstv3*, *Dub1*, *Dazl* or *Ott* did not change *Zscan4* relative expression levels (Fig. 1e). However, forced expression of *Tbx3* in mouse ES cells elevated expression levels of *Zscan4* as well as *Tcstv1*, *Tcstv3*, *Dub1* and *Dazl* (Fig. 1f). *Tcstv1*, *Tcstv3*, *Dub1* all reportedly are 2-cell specific markers and *Dazl* also up-regulated in two-cell embryos⁷. *Tbx3* was expressed in ES cells, and expressed more in *Zscan4*-EGFP positive ES cells by immunofluorescence microscopy (Fig. 1g). Previous study also showed that *Tbx3* are heterogeneously expressed in ES cell cultures by immunofluorescence^{5,14,15}. These data suggest that *Tbx3* might be a novel regulator of *Zscan4*/2C-state in mouse ES cells.

Furthermore, *Tbx3* was up-regulated in zygotes and 2-cell embryos during mouse early embryo development (Supplementary Fig. 1a), consistent with previous report that *Tbx3* was elevated in 2-cell embryos compared with oocytes⁷. We also verified that the 2-cell embryo specific genes *Zscan4*, *Tcstv1* and *Tcstv3* were elevated in 2-cell embryos, but greatly reduced after the 2-cell stage (Supplementary Fig. 1b–1d). It seemed that *Tbx3* is expressed earlier, despite at relatively lower levels, than did other 2-cell genes.

Ectopic expression of *Tbx3* activates *Zscan4*/2-cell state of mouse ES cell cultures. Transient ectopic expression of *Tbx3* up-regulates *Zscan4* (Fig. 1f). We also generated *Tbx3* stable overexpression (OE) cell lines by electroporation. Morphologically, *Tbx3* OE ES cells showed compacted cell colonies like mock ES cells electroporated with empty vector (Fig. 2a). Increased expression levels of *Tbx3* and *Zscan4* in *Tbx3* OE cells were confirmed by immunofluorescence microscopy, quantitative real time PCR and western blot (Fig. 2b–2d). To examine the dynamics of *Zscan4*⁺/2C pool upon *Tbx3* over-expression, ES cells were then sorted into *Zscan4*⁺ and *Zscan4*⁻ populations by flow cytometry. *Tbx3* over-expression only slightly increased *Zscan4*⁺/2C cell population, but notably more the fluorescence intensity of *Zscan4*⁺ cells ($p < 0.0001$) (Fig. 2e–2g). *Tbx3* overexpression did not impact the cell cycle progression (Fig. 2h), nor Oct4 expression by immunofluorescence relative quantification estimated using ImageJ software (Fig. 2i, 2j). Furthermore, ectopic expression of *Tbx3* did not alter expression of other pluripotency-associated genes by qPCR and immunofluorescence (Supplementary Fig. 2a, 2b), nor differentiation by standard *in vitro* embryoid body formation tests (Supplementary Fig. 3).

***Tbx3* plays a role in telomere length maintenance of mouse ES cells.** *Zscan4* is a specific marker for ES cells and the 2-cell embryos, and required for telomere lengthening and genomic stability of ES cells by activating telomere sister chromatid exchange (T-SCE)⁴. Remarkably, telomeres lengthened rapidly in one- to two-cell stage embryos presumably through telomere recombination or T-SCE¹⁶. Both transient and stable *Tbx3* overexpression up-regulates *Zscan4* (Fig. 1f, Fig. 2). We hypothesized that *Tbx3*-induced activation of *Zscan4*⁺/2C-state genes may function in the telomere length regulation of ES cells. By telomere quantitative fluorescence *In situ* hybridization (Q-FISH) analysis¹⁷, telomeres were significantly ($p < 0.0001$) lengthened in *Tbx3* OE ES cells compared to the mock ES cells following culture for 13 passages (83.65 ± 18.01 TFU in *Tbx3* OE1 and 82.82 ± 17.00 TFU in *Tbx3* OE2 cells vs 70.64 ± 16.49 TFU in mock ES cells) (Fig. 3a). The telomere QFISH data on telomere elongation in *Tbx3* OE ES cells was further validated by quantitative real time PCR shown as T/S ratio¹⁸ (Fig. 3b).

Expression of telomerase subunit *Tert* and *Terc* remained at similar levels between *Tbx3* OE ES cells and mock ES cells (Fig. 3c). Moreover, over-expression of *Tbx3* in WT, telomerase-null G1 or G4 ES cells¹⁹ also led to increased expression of *Zscan4* (Fig. 3d). These data suggest that *Tbx3* overexpression does not significantly increase telomerase activity and that *Tbx3* can still up-regulate *Zscan4* in ES cells without telomerase. To determine whether telomere lengths are altered in *Terc*^{-/-} ES cells by overexpressing *Tbx3*, we generated stable *Tbx3* overexpression G1 *Terc*^{-/-} ES cell lines. Expression levels of *Tbx3* and *Zscan4* were elevated in *Tbx3* overexpression G1 *Terc*^{-/-} ES cells relative to mock controls (Fig. 3e), while telomeres were notably lengthened in stable *Tbx3* overexpression G1 *Terc*^{-/-} ES cells following culture for 11 passages (Fig. 3f). Taken together, *Zscan4*-mediated telomere recombination may contribute to telomere elongation following *Tbx3* overexpression. However, we cannot exclude other possibilities responsible for telomere elongation in *Tbx3* OE ES cells, including increased accessibility of telomerase to telomeres, or up-regulation of telomeric non-coding RNAs recently shown to promote telomere elongation²⁰.

***Tbx3* regulates *Zscan4* promoter activity.** To understand potential mechanisms underlying regulation of *Zscan4* expression by *Tbx3*, we performed dual luciferase assay using the 2570 bp of full length of *Zscan4c* promoter⁴. *Zscan4c* promoter activity was significantly increased following *Tbx3* over-expression ($p < 0.0001$) (Supplementary Fig. 4a). Over-expression of *Tbx3* resulted in nearly five fold enhanced luciferase activity compared to mock controls. Coincidentally, *Tbx3* increases the expression levels of *Zscan4* in *Zscan4*⁺ cells (Fig. 2e, 2g). These data suggest that *Tbx3* might act on the *Zscan4* promoter to regulate its expression. We divided the promoter of *Zscan4c* into 7 regions (Supplementary Fig. 4b), with the initiation codon located at +811 bps⁴. The promoter activity was low in Luc1/Luc2, but rapidly increased from Luc3 and the Luc5 with full length of *Zscan4c* promoter the highest. To further narrow down possible location(s) of *Zscan4c* promoter affected by *Tbx3*, we analyzed the promoter activity following *Tbx3* overexpression. Luc1 showed increased activity resulting from *Tbx3* overexpression (Supplementary Fig. 4b), suggesting that *Tbx3* might influence +608–+811 of *Zscan4c* promoter to regulate *Zscan4* promoter activity. Luc2-Luc5 regions also exhibited increased *Zscan4* promoter activity by *Tbx3* overexpression. Luc6 and Luc7 did not contain Luc1 and Luc2, respectively, but also showed increased promoter activity after *Tbx3* overexpression, suggesting that -1759–+608 regions also might be influenced by *Tbx3* overexpression. Taken together, the full length of *Zscan4c* promoter can be influenced by *Tbx3* overexpression.

Next, we asked whether *Tbx3* as a transcription factor binds to *Zscan4* promoter regions and directly regulates *Zscan4* expression. We performed chromatin immunoprecipitation (ChIP)-qPCR in ES cells using *Tbx3* antibody and 13 primer pairs 9 kb upstream of *Zscan4c* translational initiation code and primer for subtelomere upstream of *Zscan4c* locus. Contrary to speculation, *Tbx3* was not enriched at *Zscan4c* promoter regions nor subtelomeric region upstream of *Zscan4c* locus (Supplementary Fig. 4c). Thus, *Tbx3* overexpression also did not increase *Tbx3* binding at these regions. Consistently, *Tbx3* ChIP-seq data also showed no enrichment of *Tbx3* at *Zscan4* promoter regions in mouse ES cells²¹. These data do not appear to suggest a direct regulation of *Zscan4* by *Tbx3*, although *Tbx3* over-expression influences the *Zscan4* promoter activity. *Tbx3* might indirectly activate *Zscan4*/2-cell genes.

***Tbx3* over-expression reduces DNA methylation level.** Further analysis of the up-regulated genes activated by *Tbx3* in Fig. 1f identified that some of the up-regulated genes, including *Zscan4*, *Tcstv1* and *Tcstv3* are located at subtelomeric regions, and *Zscan4* gene clusters are located at subtelomeric regions of chromosome 7. Telomeres and subtelomeres are densely compacted with repressive

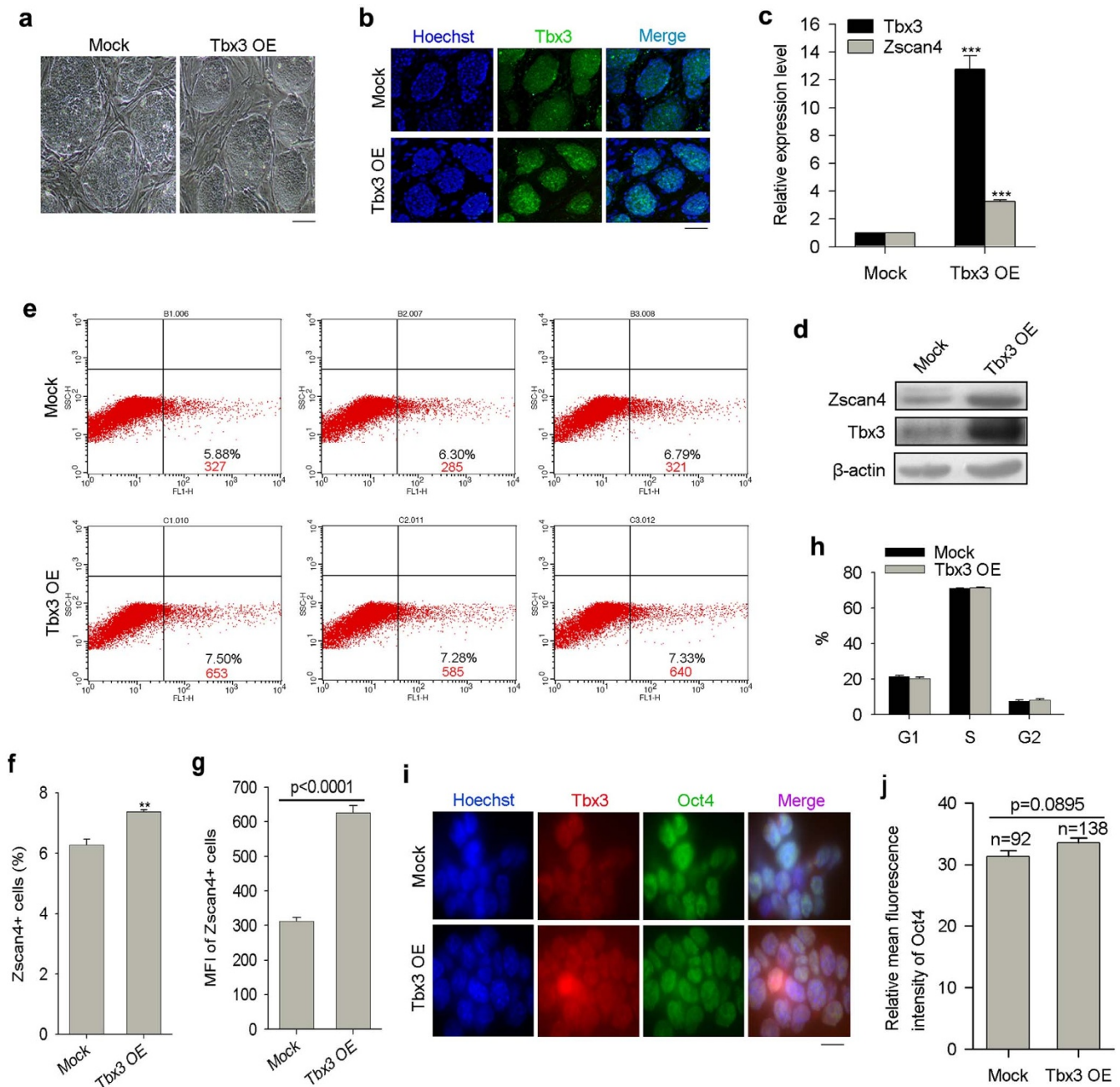


Figure 2 | *Tbx3* up-regulates *Zscan4* and maintains normal cell cycle. (a) Morphology of *Tbx3* stable over-expressed ES cells and mock ES cells. (b–d) Confirmation of the over-expression of *Tbx3* and *Zscan4* in *Tbx3* OE ES cells by immunofluorescence intensity (b), qPCR (c) and western blot (d). Full-length gel images are available in Supplementary Figure 5. ***, $p < 0.001$, compared to mocks. Scale bar = 100 μm . (e) Flow cytometry of *Zscan4*⁺ cells in transient *Tbx3* over-expression in *Zscan4*-EGFP ES cells. Percentage and mean fluorescence intensity of *Zscan4*⁺ cells are indicated. (f) *Tbx3* over-expression slightly increased proportion of *Zscan4*⁺ cells in ES cell population by FACS. **, $p < 0.01$, compared to mocks. (g) The mean fluorescence intensity (MFI) of *Zscan4*⁺ cells increased remarkably after *Tbx3* over-expression. (h) Cell cycle analysis shows no significance difference between *Tbx3* OE cells and mock ES cells. Error bars indicate mean \pm SEM ($n = 3$ or 4). (i) Co-immunostaining of *Tbx3* and Oct4 in *Tbx3* OE ES cells compared with mock ES as controls. Scale bar = 10 μm . (j) Quantification of relative mean fluorescence intensity of Oct4 estimated by ImageJ software. n , number of cells counted.

DNA methylation and histone modifications that are important regulators of mammalian telomere lengths²². The repressive H3K9me3 is detected at satellite, telomere, subtelomere and active long-terminal repeats, and can spread into proximal unique sequences²³. Mouse primary cells deficient for Suv39h1 and Suv39h2, which govern methylation of histone H3 Lys9 in heterochromatin regions, exhibit abnormal telomere lengthening and increased telomere recombination²⁴, suggesting the essential role of H3K9me3 in the negative regulation of telomere length.

Other than the repressive histone modifications, telomeric H3 and H4 histones are generally hypoacetylated^{25,26}. DNA methyltransferases (DNMTs) deficiency can lead to reduced global DNA methylation, increased telomere recombination as indicated by sister-chromatid exchanges involving telomeric sequences, and dramatic telomere elongation²⁷. These repressive DNA methylation and histone modification at subtelomeric regions form an inhibitory effect to the genes nearby, known as Telomere Position Effect (TPE)^{28,29}.

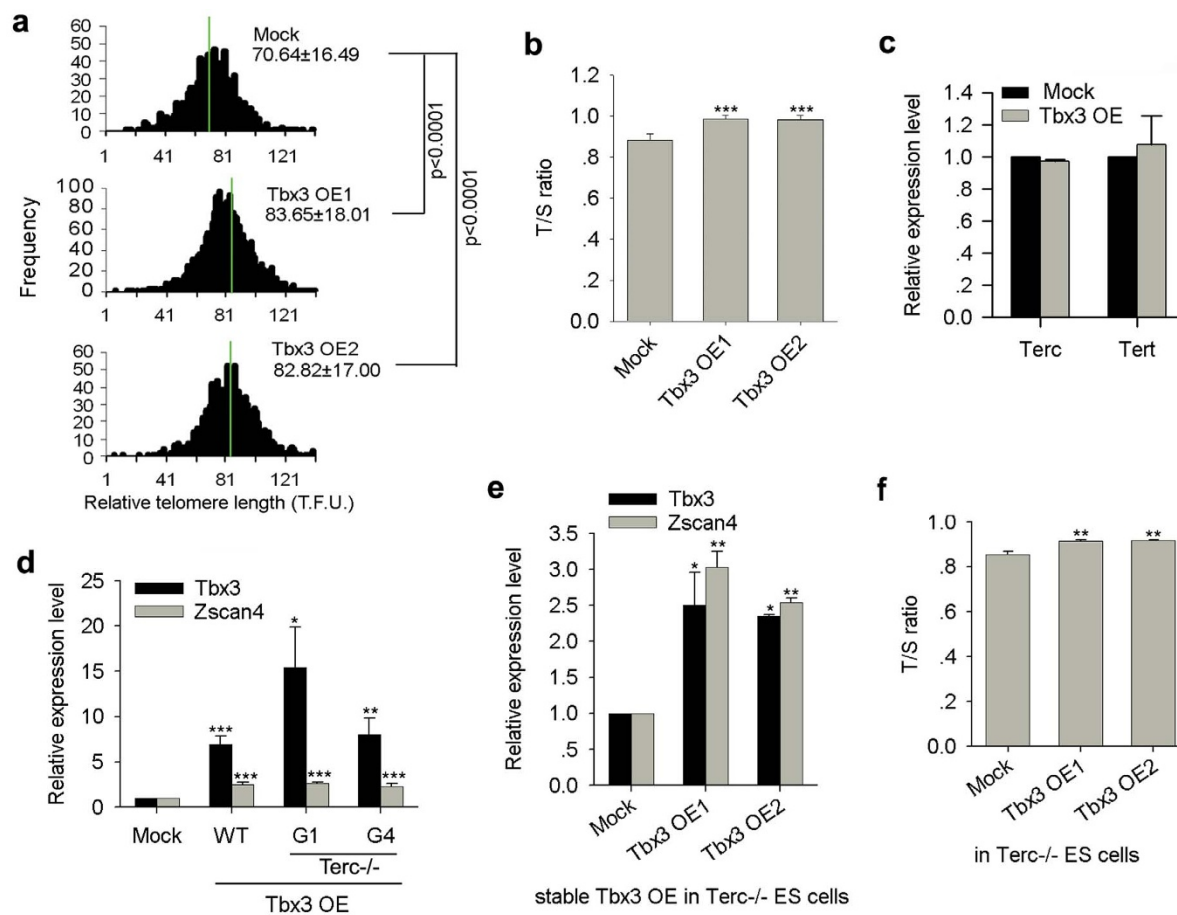


Figure 3 | *Tbx3* elongates telomeres of ES cells and up-regulates *Zscan4* in telomerase-deficient ES cells. (a) Distribution histogram showing relative telomere length of *Tbx3* overexpression (OE) ES cell lines compared to mock ES cells by telomere Q-FISH and the TFL-TELO software. TFU, arbitrary telomere fluorescence unit. Green line, median telomere length, which also is indicated on right hand corner. (b) qPCR analysis of telomere length shown as T/S ratio in *Tbx3* OE ES cells compared with mock ES cells. (c) qPCR shows no significance difference in expression levels of *Terc* and *Tert* between *Tbx3* OE ES cells and mock ES cells. (d) *Zscan4* activation by *Tbx3* over-expression is independent of telomerase involvement. *Tbx3* over-expression up-regulates *Zscan4* in WT ESC, G1 *Terc*^{-/-} ESC and G4 *Terc*^{-/-} ESC. (e) Expression levels of *Tbx3* and *Zscan4* in stable *Tbx3* OE G1 *Terc*^{-/-} ES cells by qPCR. (f) qPCR analysis of telomere length shown as T/S ratio of stable *Tbx3* OE G1 *Terc*^{-/-} ES cells compared with mock ES cells. Error bars indicate mean \pm SEM (n = 3). *, p < 0.05; **, p < 0.01; ***, p < 0.001, compared to mocks.

Tbx3 over-expression did not alter the histone modification levels of H3K9me3 and acetylated H3 (ACh3) by western blot (Fig. 4a). We then asked whether *Tbx3* inhibits DNA methylation, resulting in derepression of *Zscan4* at subtelomeres. DNA methyltransferases *Dnmt3a* and *Dnmt3b* can methylate hemimethylated and unmethylated DNA, whereas the recently discovered ten-eleven translocation (Tet) family proteins have the ability to remove methyl group in cytosine by gradual oxidization, leading to DNA demethylation^{30–32}. An elegant study clearly demonstrate that maternal origin *Dnmt3a* is notably expressed in oocytes, zygotes, 2-cell and 4-cell early mouse embryos and dramatically reduced from 8-cell stage to blastocysts, while *Dnmt3b* is undetectable in zygote and 2-cell embryos, but expressed only from 4 cell -to blastocysts³³, further supporting that *Dnmt3a* and *Dnmt3b* also exhibit non overlapping functions in development^{34,35}. *Dnmt3b* is specifically expressed in pluripotent embryonic cells, such as inner cell mass, epiblast and embryonic ectoderm cells, whilst *Dnmt3a* is significantly and ubiquitously expressed after E10.5³⁵. Minimal levels of *Dnmt3b* in zygote and 2-cell embryos coincide with activation of 2-cell genes *Zscan4*, *Tcstv1/3* and *Eif1 α* . Western blot analysis proved the decreased protein levels of *Dnmt3b* and increased levels of *Tet2* following *Tbx3* over-expression (Fig. 4a). Accordingly, DNA modification of 5-methylcytosine (5mC) was reduced and 5-hydroxymethylcytosine (5hmC) increased in *Tbx3* OE ES cells analyzed by flow cytometry (Fig. 4b,

4c), suggesting that *Tbx3* can reduce global DNA methylation levels by regulation of enzymes for methylation or demethylation. *Tbx3* is a transcriptional repressor that belongs to the *Tbx2/3/4/5* subfamily of T-box transcriptional regulators^{36,37}, and binds to 5' proximal regions of *Dnmt3a* and *Dnmt3b* by ChIP-Seq analysis (1581bp to 5' proximal of *Dnmt3a* and 6199 bp to 5' proximal of *Dnmt3b*, respectively)²¹. Furthermore, we performed ChIP-qPCR using anti-*Dnmt3b* and showed the reduced binding of *Dnmt3b* to *Zscan4* promoter regions, *Tcstv1* and *Tcstv3* promoter locus, as well as subtelomeres of chromosome 7 following *Tbx3* overexpression (Fig. 4d). Finally, knockdown of *Dnmt3b* with different shRNA sequences raised the protein levels of *Zscan4* in ES cells (Fig. 4e, 4f). These data suggest that *Tbx3* represses *Dnmt3b* (and possibly *Dnmt3a*), reducing DNA methylation level and leading to up-regulation of *Zscan4*.

Discussion

Our data show that *Tbx3* activates *Zscan4*^{+/2C}-state in mouse ES cells likely by reducing global DNA methylation level, which in turn leads to derepression of genes at subtelomeres, including *Zscan4* and *Tcstv1/3*. Telomere length maintenance by *Zscan4*, despite that the precise underlying mechanism remains elusive, is critical for unlimited self-renewal and pluripotency of ES/iPS cells^{4,15,17}. *Dnmt3b* preferentially targets to repetitive sequences³⁸, and is specifically required for methylation of pericentromeric minor satellite repeats³⁴ and also

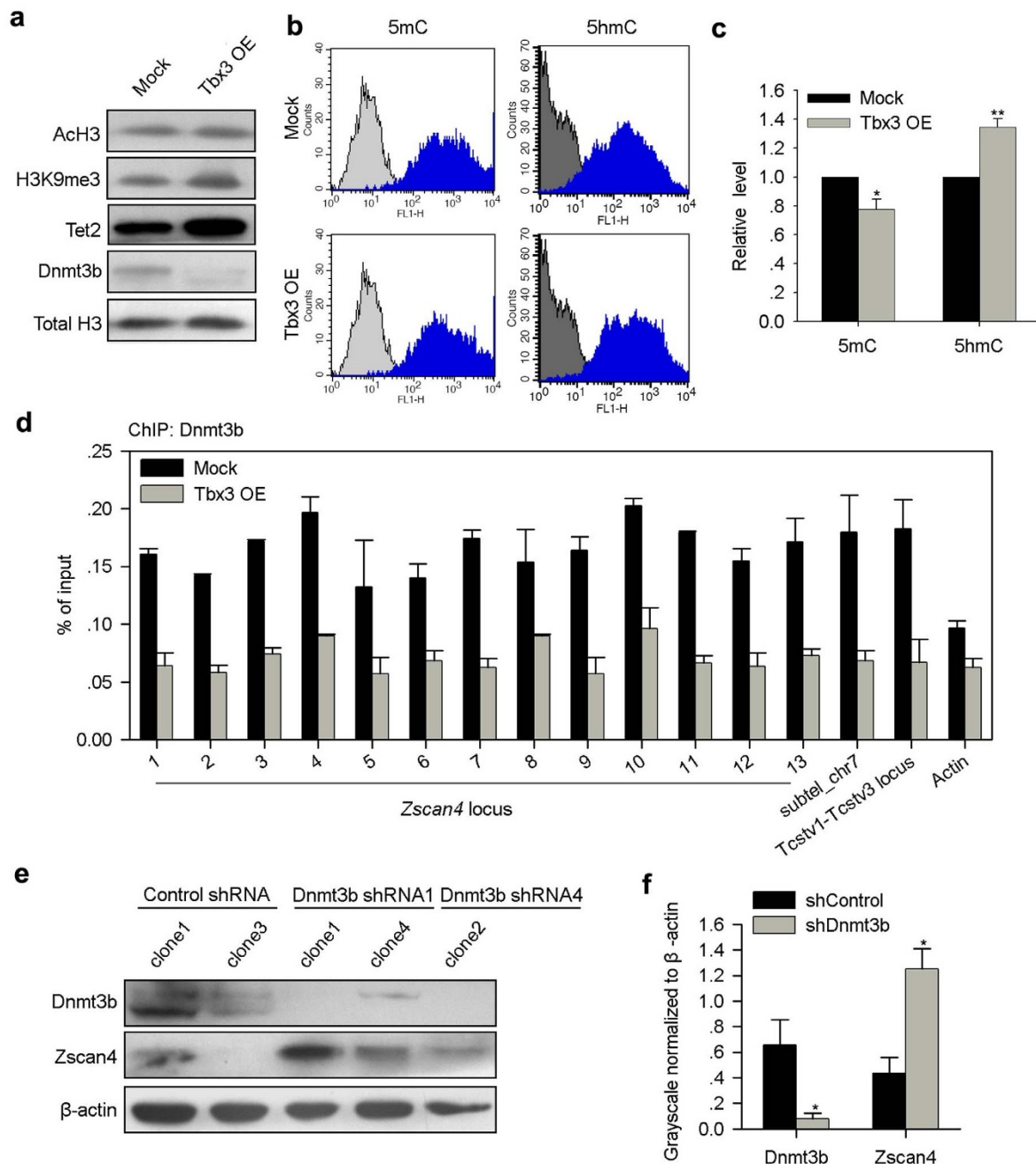


Figure 4 | *Tbx3* reduces global DNA methylation of ES cells. (a) *Tbx3* over-expression did not change levels of H3K9me3 and AcH3 but reduced Dnmt3b and increased Tet2 protein levels. Full-length gel images are available in Supplementary Figure 5. (b) Global DNA 5-methylcytosine/5-hydroxymethylcytosine level in *Tbx3* OE ES cells and mock ES cells by specific labeling with anti-5-MeC and 5hmC antibodies analyzed by flow cytometry. (c) Relative 5-methylcytosine/5-hydroxymethylcytosine level in *Tbx3* OE ES cells compared with mock ES cells. The fluorescence intensity for mock ES cells was arbitrarily set as 1, and the fluorescence intensity of *Tbx3* OE ES cells was expressed relative to mock ES cells. *, $p < 0.05$; **, $p < 0.01$, compared to mocks. Error bars indicate mean \pm SEM ($n = 3$). (d) ChIP-qPCR assay of Dnmt3b binding on proximal *Zscan4* and *Tcstv1-Tcstv3* promoters, and subelomere of chromosome 7 in mock and *Tbx3* OE ES cells. Error bars indicate mean \pm SEM ($n = 2$). (e) Dnmt3b knockdown increased *Zscan4* protein level in ES cells. Two different Dnmt3b RNAi sequences were used. (f) Relative protein quantity normalized to β -actin by Bio-Rad Quantity One software.

telomere repeats^{39,40}. Subtelomeric regions are CG-rich and contain repetitive sequences^{41,42}. *Zscan4* promoter activity was activated by *Tbx3*. However, no direct binding to *Zscan4* promoter was found for *Tbx3*, and this data is consistent with the ChIP-seq data²¹. We find that *Tbx3* appears to inhibit *Dnmt3b* and reduce DNA methylation, indirectly regulating genes located in repetitive sequences including *Zscan4* at subtelomeres, which contributes to telomere recombination and elongation, providing evidence supporting telomere

position effects influenced by *Tbx3*. A speculative model on the role of *Tbx3* in epigenetic regulation of telomere length in ES cells is proposed in Figure 5.

Tbx3 belongs to T-box (TBX) transcription factors family⁴³, is known to function generally as a transcriptional repressor, although *Tbx3* has also been shown to have an activation domain^{44,45}. *Tbx3* mediates the leukemia inhibitory factor (LIF) signaling to core circuitry of pluripotency in mouse ES cells¹⁴. Phosphoinositide 3-kinase

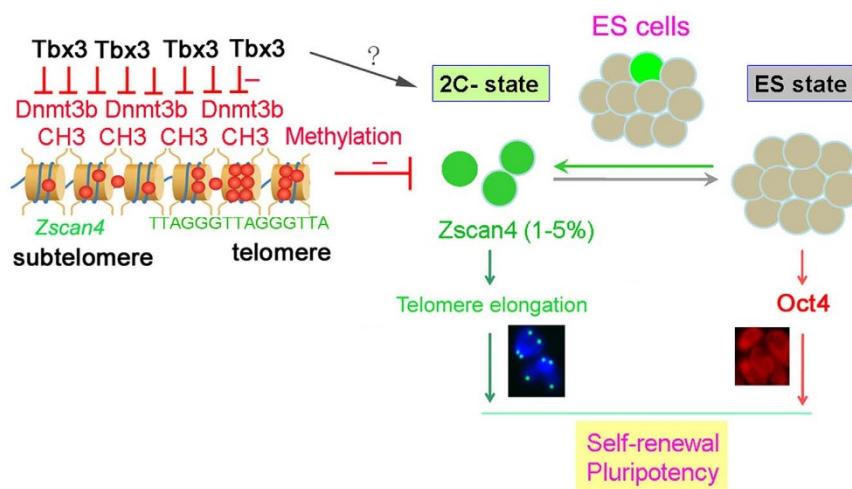


Figure 5 | A speculative model for role of *Tbx3* in ES cell cultures by epigenetic regulation of *Zscan4*/2C-state. *Tbx3* plays a novel role in maintaining self-renewal and pluripotency of mouse ES cells. *Tbx3* represses *Dnmt3b*, reduces DNA methylation and increases hypomethylation, de-repressing genes at repeated sequences, including *Zscan4* at subtelomeres, which contributes to telomere elongation and self-renewal of ES cells. (?) *Tbx3* also may regulate *Zscan4*/2C state and telomeres via other mechanisms that remain to be identified.

(PI3K)-dependent signaling has been implicated in the regulation of ES cell fate¹⁵. *Tbx3*, *Zscan4* and *Nanog* are all regulated by PI3K signaling pathway^{14,15}. *Zscan4* and *Nanog* are decreased within 24 h following PI3K inhibition by LY294002 treatment, while *Tbx3* is decreased after 48 h treatment¹⁵, demonstrating that *Tbx3* is delayed in response to PI3K inhibition compared to *Nanog* and *Zscan4*. *Tbx3* acts upstream of *Nanog* in PI3K pathway to mediate LIF independent self-renewal¹⁴, and *Tbx3* over-expression up-regulates *Zscan4*, suggesting that *Zscan4* may be downstream target of *Tbx3* in PI3K signaling pathway.

Notably, *Tbx3* enhances reprogramming efficiency and quality of iPS cells²¹. Expression of *Tbx3* is directly repressed by binding of Tcf3 to its promoter and up-regulated by Tcf3 knockdown²¹. Furthermore, Tcf3 depletion increases somatic cell reprogramming⁴⁶. Interestingly, *Zscan4* enhances the reprogramming efficiency, promotes genomic stability during reprogramming and dramatically improves the quality of iPS cells as demonstrated by tetraploid complementation^{11,12}. We found a novel role for *Tbx3* in regulation of ES pluripotency and self-renewal by regulating 2C-state and *Zscan4* expression that may elongate telomeres by recombination. *Tbx3* reduces *Dnmt3b* and increases *Tet2* levels, which synergistically results in reduced DNA methylation level, and elevated *Zscan4* promoter activity and gene expression. It has been shown that *Dnmt3b* and DNA methylation block iPS induction^{47–49}, whereas *Tet2* and hypomethylation facilitates iPS generation^{50,51}. It is possible that reduced levels of DNA methylation together with increased expression of *Zscan4* and other 2C genes induced by *Tbx3* also may contribute to enhanced iPS reprogramming efficiency and improved iPS cell quality through activation of *Zscan4*/2C genes during reprogramming.

Tbx3 plays critical roles in mouse embryogenesis and ES cell fate decision⁵². *Tbx3*-deficient embryos have limb defects and fail to form mammary glands, and die between E12.5 and E15.5^{44,53,54}. *Tbx3* is upregulated during early embryo development and involved in telomere length maintenance. Telomere length was associated with authentic pluripotency of ES/iPS cells¹⁹. Telomeres are critical for highly proliferative cell types and organs, and telomere shortening leads to defective embryonic development.

In addition to its key roles in embryonic development, *TBX3* also is implicated in tumorigenesis. *TBX3* was shown to be over-expressed in variety types of cancers and implicated in cancer stem cell proliferation and metastasis, including breast, ovarian, pancreas, melanoma, liver, cervical and lung cancers³⁶. Telomere maintenance also is critical for cancer growth and metastasis^{55,56}, and telomere

has been a target for cancer therapy. Using ES cell model, we suggest that *Tbx3* plays a novel role in promoting telomere elongation by epigenetic regulation and activation of *Zscan4*.

Methods

Mouse ES cells. BF10 and F1 ES cell lines derived from B6C3F1 mice, and early and late generation telomerase-deficient ES cells and control ES cells were generated and characterized as described previously^{19,57}. J1 ES cells were cultured without feeder. The ES cell culture medium consisted of knock-out DMEM (Gibco) with 15% FBS (Hyclone), 1000 U/ml mouse leukemia inhibitory factor (LIF) (ESGRO, Chemicon), 0.1 mM non-essential amino acids, 0.1 mM β -mercaptoethanol, 1 mM L-glutamine, and penicillin (100 U/ml) and streptomycin (100 μ g/ml). For culture of ES cell lines, the medium was changed daily, and cells routinely were passaged every two days. Animals were cared for and treated according to guidelines set by U.S. National Research Council and the use of mice for the research approved by Nankai Animal Care and Use Committee.

Vector construction. Murine *Tctv1*, *Tctv3*, *Ott* and *Tbx3* CDS were cloned into expression vector pCAGIpuro; murine *Zscan4c* CDS was cloned into pCMV-Tag2B and *Dazl* CDS was cloned into pEF6 expression vector. A putative *Zscan4c* promoter containing the 2570 bp upstream sequences from the *Zscan4c* start codon⁴, was amplified from mouse F1 ES cell genomic DNA with TransStar Fastpfu polymerase (Transgene) using the following primers: forward: AGAGATGCTTCTGCATCTGT; reverse: TGTGGTGACAATGGTGTGAAAG. The PCR product was inserted into pEGFP-1 vector at Sall/KpnI sites. The 2570 full length putative *Zscan4c* promoter was then cut using SacI/SmaI from pEGFP-1-*Zscan4c* and inserted into pGL3-basic vector containing several base pairs from pEGFP-1 vector. The other six *Zscan4* promoter fragments were amplified from the full length *Zscan4* promoter and inserted into pGL3-basic vector at KpnI/Sall sites.

Generation of *Tbx3* OE, p*Zscan4*-EGFP and stable *Dnmt3b* knockdown ES cells. BF10 ES cells were transfected by electroporation with pCAGIpuro-*Tbx3* expression vector or empty vector served as control, and selected with 1.5 μ g/ml puromycin for two weeks to achieve stable *Tbx3* over-expression or mock ES cell lines. G1 *Terc*^{-/-} ES cells were infected with pMSCV-*Tbx3* overexpression or control retrovirus, selected with G418, and clones were picked for further experimental analysis. The pEGFP-1-*Zscan4* vector was linearized by Xho I digestion and purified by PCR purification kit (Transgene). Feeder-free J1 ES cells were transfected with 2 μ g linearized vector using lipofectamine 2000 (Invitrogen) and selected with 400 μ g/ml G418 (Invitrogen) for 2 weeks, and a clone with bright green fluorescence was picked and expanded for further experiments. *Zscan4*-EGFP ES cells were sorted by fluorescence-activated cell sorting using BD FACSAria. The sorted *Zscan4*⁺ (positive) and *Zscan4*⁻ (negative) ES cells were used for RNA extraction. Control and two different shRNA sequences against *Dnmt3b* mRNA were used for *Dnmt3b* knockdown experiment. The sequences were cloned into pSIREN-RetroQ (Clontech) with puromycin replaced by neomycin and the resultant vectors introduced into Plat-E cells to package retrovirus. Feeder-free J1 ES cells were then infected with control and *Dnmt3b* RNAi retrovirus, ES cells were then selected with 500 μ g/ml G418 for about 10 days and the resistant clones were picked. The RNAi sequences were as following:

Control shRNA forward:
 GATCCGCGTTC AATTAGCAGACCATTCAAGAGATGGTCTGCTAATTG
 AACCCCTTTTAAAGCTTG;



reverse:

AATTCAGCTTAAAAAGCGTTCAATTAGCAGACCATCTCTGAATGG
TCTGCTAATTGAACGCCG.

Dnmt3b shRNA1 forward:

GATCCGGAGTTGGGTATTAAGTGTTCAGAGACACTTAATACCCA
ACTCCTTTTTTAAGCTTG;

Reverse:

AATTCAGCTTAAAAAGGAGTTGGGTATTAAGTGTCTCTTGAACAC
TTTAATACCAACTCCG.

Dnmt3b shRNA4 forward:

GATCCGTTGAAGTAGGTAGTAAAGATGTTCAAGAGACATCTTACTACC
TACTTCAAGCTTTTTTAAGCTTG.

Reverse:

AATTCAGCTTAAAAAGCTTGAAGTAGGTAGTAAAGATGTTCTTGA
CATCTTACTACTTCAAGCG.

FACS analysis of Zscan4 positive ES cells. 1×10^5 Zscan4-EGFP J1 ES cells per 12-well were transfected with 1 μ g mock or *Tbx3* over-expression (OE) vector, and analyzed for percentage of *Zscan4* positive cells 48 h later by FACS.

Luciferase reporter assay. 1×10^5 feeder-free J1 ES cells per 24 well were transfected with 0.8 μ g pGL3-Zscan4c vector (containing Luc1 to Luc7) and 8 ng pRL-SV40 vector (as control) and 1 μ g mock or *Tbx3* over-expression vector using lipofectamine 2000 (Invitrogen) according to manufacturer's instructions. Transfected J1 ES cells were lysed 24 h later with $1 \times$ PLB (positive lysis buffer, Promega), shaken for 15 min, and then centrifuged at 13000 rpm for 10 min at 4°C. The supernatants were collected and analyzed for luciferase activity by dual reporter assay according to manufacturer's instructions.

Immunofluorescence microscopy. Cells were washed twice in phosphate buffered saline (PBS), then fixed in freshly prepared 3.7% paraformaldehyde in PBS (pH 7.4) for 15 min on ice cube, permeabilized in 0.1% Triton X-100 in blocking solution (3% goat serum plus 0.5% BSA in PBS) for 30 min at room temperature, washed three times (each for 15 min), and left in blocking solution for 1 h. Cells were incubated overnight at 4°C with primary antibodies against *Tbx3* (sc-31657, Santa Cruz), Nanog (ab80892, Abcam), Oct4 (sc5279, Santa Cruz), SMA (ab5694-100, Abcam), AFP (DAK-N1501, DAKO), Nestin (ab6142, Abcam), washed three times (each for 15 min), and incubated for 1 h with secondary antibodies, bovine anti-goat IgG-FITC (sc2348, Santa Cruz), Alexa Fluor 594 donkey anti-goat IgG (A-11058, MP), Alexa Fluor 568 Goat anti-rabbit (A-11011, MP), or Alexa Fluor 488 Goat anti-mouse (A-11001, MP), diluted 1:200 with blocking solution. Samples were washed, and counterstained with 0.5 μ g/ml Hoechst33342 (H1398, MP) in Vectashield mounting medium. Fluorescence was detected and imaged using a fluorescence microscope (Zeiss Axio Imager Z1).

Telomere quantitative fluorescence in situ hybridization (QFISH). Telomere length and function (telomere integrity and chromosome stability) was estimated by QFISH. Cells were incubated with 0.5 μ g/ml nocodazole for 1.5 h to enrich cells at metaphases. Chromosome spreads were made by a routine method. Metaphase-enriched cells were exposed to hypotonic treatment with 75 mM KCl solution, fixed with methanol: glacial acetic acid (3:1) and spread onto clean slides. Telomere FISH and quantification were performed as described previously⁵⁸, except for FITC-labeled (CCCTAA) peptide nucleic acid (PNA) probe used in this study. Telomeres were denatured at 80°C for 3 min and hybridized with telomere specific PNA probe (0.5 μ g/ml) (Panagene, Korea). Chromosomes were counter-stained with 0.5 μ g/ml DAPI. Fluorescence from chromosomes and telomeres was digitally imaged on a Zeiss microscope with FITC/DAPI filters, using AxioCam and AxioVision software 4.6. For quantitative measurement of telomere length, telomere fluorescence intensity was integrated using the TFL-TELO program (gift kindly provided by P. Lansdorp, Terry Fox Laboratory, Vancouver, Canada), and calibrated using standard fluorescence beads.

Telomere measurement by quantitative real-time PCR. Cells were washed in PBS and stored at -20°C until subsequent DNA extraction. Genome DNA was prepared using DNeasy Blood & Tissue Kit (Qiagen, Valencia, CA). Average telomere length was measured from total genomic DNA using a real-time PCR assay, modified for measurement of mouse telomeres¹⁸. PCR reactions were performed on the iCycler iQ real-time PCR detection system (Bio-Rad, Hercules, CA), using telomeric primers, primers for the reference control gene (mouse 36B4 single copy gene) (Table S2) and PCR settings as previously described¹⁶. For each PCR reaction, a standard curve was made by serial dilutions of known amounts of DNA. The telomere signal was normalized to the signal from the single copy gene to generate a T/S ratio indicative of relative telomere length. Equal amounts of DNA were used for each reaction.

Gene expression analysis by quantitative real-time PCR. Total RNA was isolated from cells using RNeasy mini kit (Qiagen). 2 μ g of RNA were subjected to cDNA synthesis using M-MLV Reverse Transcriptase (Invitrogen). Real-time quantitative PCR reactions were set up in duplicate with the FastStart Universal SYBR Green Master (ROX) (Roche) and run on the iCycler iQ5 2.0 Standard Edition Optical System (Bio-Rad). Each sample was repeated 3 times and analyzed with β -actin as the internal control. Most primers were designed using the IDT DNA website (<http://www.idtdna.com/Home/Home.aspx>). The primers used are in Table S1.

Global DNA methylation analysis. DNA methylation was analyzed by immunostaining with 5-MeC (NA81, Calbiochem) and 5hmC (39769, active motif) antibodies as previously described^{59,60}. ES cells were dissociated in trypsin-EDTA and washed in PBS twice and fixed in ice-cold 3.7% PFA for 30 min, washed in 0.05% PBT, permeabilized in 0.2% Triton X-100 solution for 30 min. Then, cells were depurinated in 4N HCl, 0.1% Triton X-100 for 10 min, washed, and then blocked in 2% BSA in PBT. Samples were incubated with anti-5-MeC or anti-5hmC antibody overnight at 4°C, washed and then incubated with FITC conjugated goat anti-mouse IgG (A-11001, Molecular Probes) or FITC conjugated anti-rabbit IgG (554020, BD Biosciences) in blocking solution for 1 h at RT, washed, and then ES cells were placed in the fluorescence-activated cell sorting for analysis and sorting by flow cytometry (BD Biosciences). Cells with immunostaining only with normal IgG antibody served as negative controls. Fluorescence distribution and intensity of cell populations following immunostaining with anti-5-MeC and 5hmC antibodies were quantified by FACS analysis. The fluorescence intensity for mock ES cells was arbitrarily set as 1, and the fluorescence intensity of *Tbx3* OE ES cells expressed relative to that of mock ES cells.

Western blot. Cells were washed twice in PBS, collected, lysed and boiled in SDS Sample Buffer at 99°C for 5 min; 35 μ g total proteins of each cell extracts were resolved by 10–12% Bis-Tris SDS-PAGE and transferred to polyvinylidene difluoride membrane (PVDF, Millipore). Nonspecific binding was blocked by incubation in 5% skim milk in TBST at room temperature for 1–2 h. Blots were then probed with various primary antibodies, *Tbx3* (sc-31657, Santa Cruz), *Zscan4* (custom-made), Dnmt3b (ab13604, Abcam), Tet2 (kind gift from Jinsong Li at SIBS), Histone H3 (ab1791, Abcam), H3K9me3 (07-442, Millipore), AcH3 (06-599, Millipore) and β -actin (P30002, Abmart) by overnight incubation at 4°C in 5% skim milk in TBST. Immunoreactive bands were then probed for 1–2 h at room temperature with the appropriate horseradish peroxidase-conjugated secondary anti-Rabbit IgG -HRP (GE Healthcare, NA934V), or anti-mouse IgG-HRP (Santa Cruz, sc-2031), or anti-goat IgG-HRP (Santa Cruz, sc-2020). The protein bands were detected by Enhanced ECL AmershamTM prime western blotting detection reagent (GE Healthcare, RPN2232).

ChIP-qPCR analysis. Mock and *Tbx3* OE ES cells (each 3×10^7) were used for ChIP experiment. Briefly, cells were fixed with freshly prepared 1% paraformaldehyde for 10 min at room temperature. Cells were harvested and their nuclei extracted, lysed, and sonicated. DNA fragments were then enriched by immunoprecipitation with 8 μ g *Tbx3* antibody (sc31657, Santa Cruz) and 4 μ g Dnmt3b antibody (ab13604, Abcam), respectively. The eluted protein:DNA complex was reverse-crosslinked at 65°C overnight. DNA was recovered after proteinase and RNase A treatment. ChIP-enriched DNA was analyzed by real-time PCR using primers for *Zscan4c* loci, subtelomeres (Table S3). β -actin served as negative control.

Statistical analysis. Percentage data and other number were analyzed by analysis of variance (ANOVA), and means were compared by Fisher's protected least-significant difference (PLSD) test using StatView software from SAS Institute Inc. (Cary, NC). Significant differences were defined as $p < 0.05$, 0.01, or lower.

1. Carter, M. G. *et al.* An in situ hybridization-based screen for heterogeneously expressed genes in mouse ES cells. *Gene Expr Patterns* **8**, 181–198 (2008).
2. Niwa, H. How is pluripotency determined and maintained? *Development* **134**, 635–646 (2007).
3. Boyer, L. A., Mathur, D. & Jaenisch, R. Molecular control of pluripotency. *Curr Opin Genet Dev* **16**, 455–462 (2006).
4. Zalzman, M. *et al.* Zscan4 regulates telomere elongation and genomic stability in ES cells. *Nature* **464**, 858–863 (2010).
5. Lanner, F. *et al.* Heparan sulfation-dependent fibroblast growth factor signaling maintains embryonic stem cells primed for differentiation in a heterogeneous state. *Stem Cells* **28**, 191–200 (2010).
6. Yoshikawa, T. *et al.* High-throughput screen for genes predominantly expressed in the ICM of mouse blastocysts by whole mount in situ hybridization. *Gene Expr Patterns* **6**, 213–224 (2006).
7. Macfarlan, T. S. *et al.* Embryonic stem cell potency fluctuates with endogenous retrovirus activity. *Nature* **487**, 57–63 (2012).
8. Surani, A. & Tischler, J. Stem cells: a sporadic super state. *Nature* **487**, 43–45 (2012).
9. Falco, G. *et al.* Zscan4: a novel gene expressed exclusively in late 2-cell embryos and embryonic stem cells. *Dev Biol* **307**, 539–550 (2007).
10. Sander, T. L. *et al.* The SCAN domain defines a large family of zinc finger transcription factors. *Gene* **310**, 29–38 (2003).
11. Jiang, J. *et al.* Zscan4 promotes genomic stability during reprogramming and dramatically improves the quality of iPSC cells as demonstrated by tetraploid complementation. *Cell Res* **23**, 92–106 (2013).
12. Hirata, T. *et al.* Zscan4 transiently reactivates early embryonic genes during the generation of induced pluripotent stem cells. *Sci Rep* **2**, 208 (2012).
13. Amano, T. *et al.* Zscan4 restores the developmental potency of embryonic stem cells. *Nat Commun* **4**, 1966 (2013).
14. Niwa, H., Ogawa, K., Shimamoto, D. & Adachi, K. A parallel circuit of LIF signalling pathways maintains pluripotency of mouse ES cells. *Nature* **460**, 118–122 (2009).



15. Storm, M. P. *et al.* Characterization of the phosphoinositide 3-kinase-dependent transcriptome in murine embryonic stem cells: identification of novel regulators of pluripotency. *Stem Cells* **27**, 764–775 (2009).
16. Liu, L. *et al.* Telomere lengthening early in development. *Nat Cell Biol* **9**, 1436–1441 (2007).
17. Wang, F. *et al.* Molecular insights into the heterogeneity of telomere reprogramming in induced pluripotent stem cells. *Cell Res* **22**, 757–768 (2012).
18. Callicott, R. J. & Womack, J. E. Real-time PCR assay for measurement of mouse telomeres. *Comp Med* **56**, 17–22 (2006).
19. Huang, J. *et al.* Association of telomere length with authentic pluripotency of ES/iPS cells. *Cell Res* **21**, 779–792 (2011).
20. Cusanelli, E., Romero, C. A. & Chartrand, P. Telomeric Noncoding RNA TERRA Is Induced by Telomere Shortening to Nucleate Telomerase Molecules at Short Telomeres. *Mol Cell* **51**, 780–791 (2013).
21. Han, J. *et al.* Tbx3 improves the germ-line competency of induced pluripotent stem cells. *Nature* **463**, 1096–1100 (2010).
22. Blasco, M. A. The epigenetic regulation of mammalian telomeres. *Nat Rev Genet* **8**, 299–309 (2007).
23. Mikkelsen, T. S. *et al.* Genome-wide maps of chromatin state in pluripotent and lineage-committed cells. *Nature* **448**, 553–560 (2007).
24. Garcia-Cao, M., O'Sullivan, R., Peters, A. H., Jenuwein, T. & Blasco, M. A. Epigenetic regulation of telomere length in mammalian cells by the Suv39h1 and Suv39h2 histone methyltransferases. *Nat Genet* **36**, 94–99 (2004).
25. Benetti, R., Garcia-Cao, M. & Blasco, M. A. Telomere length regulates the epigenetic status of mammalian telomeres and subtelomeres. *Nat Genet* **39**, 243–250 (2007).
26. Wong, L. H. Epigenetic regulation of telomere chromatin integrity in pluripotent embryonic stem cells. *Epigenomics* **2**, 639–655 (2010).
27. Gonzalo, S. *et al.* DNA methyltransferases control telomere length and telomere recombination in mammalian cells. *Nat Cell Biol* **8**, 416–424 (2006).
28. Ottaviani, A., Gilson, E. & Magdinier, F. Telomeric position effect: from the yeast paradigm to human pathologies? *Biochimie* **90**, 93–107 (2008).
29. Slijepcevic, P. Telomere length regulation—a view from the individual chromosome perspective. *Exp Cell Res* **244**, 268–274 (1998).
30. He, Y. F. *et al.* Tet-mediated formation of 5-carboxylcytosine and its excision by TDG in mammalian DNA. *Science* **333**, 1303–1307 (2011).
31. Ito, S. *et al.* Role of Tet proteins in 5mC to 5hmC conversion, ES-cell self-renewal and inner cell mass specification. *Nature* **466**, 1129–1133 (2010).
32. Ito, S. *et al.* Tet proteins can convert 5-methylcytosine to 5-formylcytosine and 5-carboxylcytosine. *Science* **333**, 1300–1303 (2011).
33. Hirasawa, R. *et al.* Maternal and zygotic Dnmt1 are necessary and sufficient for the maintenance of DNA methylation imprints during preimplantation development. *Genes Dev* **22**, 1607–1616 (2008).
34. Okano, M., Bell, D. W., Haber, D. A. & Li, E. DNA methyltransferases Dnmt3a and Dnmt3b are essential for de novo methylation and mammalian development. *Cell* **99**, 247–257 (1999).
35. Watanabe, D., Suetake, I., Tada, T. & Tajima, S. Stage- and cell-specific expression of Dnmt3a and Dnmt3b during embryogenesis. *Mech Dev* **118**, 187–190 (2002).
36. Lu, J., Li, X. P., Dong, Q., Kung, H. F. & He, M. L. TBX2 and TBX3: the special value for anticancer drug targets. *Biochim Biophys Acta* **1806**, 268–274 (2010).
37. Rallis, C., Del Buono, J. & Logan, M. P. Tbx3 can alter limb position along the rostrocaudal axis of the developing embryo. *Development* **132**, 1961–1970 (2005).
38. Chen, T. & Li, E. Structure and function of eukaryotic DNA methyltransferases. *Curr Top Dev Biol* **60**, 55–89 (2004).
39. Deng, Z., Campbell, A. E. & Lieberman, P. M. TERRA, CpG methylation and telomere heterochromatin: lessons from ICF syndrome cells. *Cell Cycle* **9**, 69–74 (2010).
40. Yehezkel, S., Segev, Y., Viegas-Pequignot, E., Skorecki, K. & Selig, S. Hypomethylation of subtelomeric regions in ICF syndrome is associated with abnormally short telomeres and enhanced transcription from telomeric regions. *Hum Mol Genet* **17**, 2776–2789 (2008).
41. Brock, G. J., Charlton, J. & Bird, A. Densely methylated sequences that are preferentially localized at telomere-proximal regions of human chromosomes. *Gene* **240**, 269–277 (1999).
42. de Lange, T. *et al.* Structure and variability of human chromosome ends. *Mol Cell Biol* **10**, 518–527 (1990).
43. Papaioannou, V. E. & Silver, L. M. The T-box gene family. *Bioessays* **20**, 9–19 (1998).
44. Davenport, T. G., Jerome-Majewska, L. A. & Papaioannou, V. E. Mammary gland, limb and yolk sac defects in mice lacking Tbx3, the gene mutated in human ulnar mammary syndrome. *Development* **130**, 2263–2273 (2003).
45. He, M., Wen, L., Campbell, C. E., Wu, J. Y. & Rao, Y. Transcription repression by Xenopus ET and its human ortholog TBX3, a gene involved in ulnar-mammary syndrome. *Proc Natl Acad Sci U S A* **96**, 10212–10217 (1999).
46. Lluis, F. *et al.* T-cell factor 3 (Tcf3) deletion increases somatic cell reprogramming by inducing epigenome modifications. *Proc Natl Acad Sci U S A* **108**, 11912–11917 (2011).
47. Guo, X. *et al.* microRNA-29b is a novel mediator of Sox2 function in the regulation of somatic cell reprogramming. *Cell Res* **23**, 142–156 (2013).
48. Huangfu, D. *et al.* Induction of pluripotent stem cells by defined factors is greatly improved by small-molecule compounds. *Nat Biotechnol* **26**, 795–797 (2008).
49. Shi, Y. *et al.* Induction of pluripotent stem cells from mouse embryonic fibroblasts by Oct4 and Klf4 with small-molecule compounds. *Cell Stem Cell* **3**, 568–574 (2008).
50. Costa, Y. *et al.* NANOG-dependent function of TET1 and TET2 in establishment of pluripotency. *Nature* **495**, 370–374 (2013).
51. Doerge, C. A. *et al.* Early-stage epigenetic modification during somatic cell reprogramming by Parp1 and Tet2. *Nature* **488**, 652–655 (2012).
52. Weidgang, C. E. *et al.* TBX3 directs cell-fate decision toward mesendoderm. *Stem Cell Reports* **1**, 248–265 (2013).
53. Hoogaars, W. M. *et al.* Tbx3 controls the sinoatrial node gene program and imposes pacemaker function on the atria. *Genes Dev* **21**, 1098–1112 (2007).
54. Bamshad, M. *et al.* The spectrum of mutations in TBX3: Genotype/Phenotype relationship in ulnar-mammary syndrome. *Am J Hum Genet* **64**, 1550–1562 (1999).
55. Blasco, M. A. Telomeres and human disease: ageing, cancer and beyond. *Nat Rev Genet* **6**, 611–622 (2005).
56. Xu, L., Li, S. & Stohr, B. A. The role of telomere biology in cancer. *Annu Rev Pathol* **8**, 49–78 (2013).
57. Chen, Z. *et al.* Birth of parthenote mice directly from parthenogenetic embryonic stem cells. *Stem Cells* **27**, 2136–2145 (2009).
58. Poon, S. S., Martens, U. M., Ward, R. K. & Lansdorp, P. M. Telomere length measurements using digital fluorescence microscopy. *Cytometry* **36**, 267–278 (1999).
59. Li, C. *et al.* Correlation of expression and methylation of imprinted genes with pluripotency of parthenogenetic embryonic stem cells. *Hum Mol Genet* **18**, 2177–2187 (2009).
60. Santos, F., Hendrich, B., Reik, W. & Dean, W. Dynamic reprogramming of DNA methylation in the early mouse embryo. *Dev Biol* **241**, 172–182 (2002).

Acknowledgments

We thank Dr. Peter Lansdorp for the TFL-TELO software. This work was supported by China MOST National Major Basic Research Program (2012CB911202, 2011CBA01002), National Natural Science Foundation of China (31271587), and Natural Science Foundation of Tianjin (12JCZDJC24800).

Author contributions

J.D., M.L., M.O., X.Y., J.Y. and J.L. performed experiments and data analysis. J.D. designed the experiments and wrote the manuscript; L.L. designed and advised the experiments, and revised manuscripts.

Additional information

Supplementary information accompanies this paper at <http://www.nature.com/scientificreports>

Competing financial interests: The authors declare no competing financial interests.

How to cite this article: Dan, J.M. *et al.* Roles for Tbx3 in regulation of two-cell state and telomere elongation in mouse ES cells. *Sci. Rep.* **3**, 3492; DOI:10.1038/srep03492 (2013).



This work is licensed under a Creative Commons Attribution-NonCommercial-NoDerivs 3.0 Unported license. To view a copy of this license, visit <http://creativecommons.org/licenses/by-nc-nd/3.0>